Spin-Peierls transition of the quasi-one-dimensional electronic system $(DMe\text{-}DCNQI)_2M$ $(M=Li,Ag)$ probed by heat capacity

Yasuhiro Nakazawa,[1,*] Akane Sato,[1,†] Mitsuro Seki,[1] Kazuya Saito,[1] Ko-ichi Hiraki,[2] Toshihiro Takahashi,[2] Kazushi Kanoda,[3] and Michio Sorai[1]

[1]*Research Center for Molecular Thermodynamics, Osaka University, Machikaneyama 1-1, Toyonaka, Osaka 560-0043, Japan*

[2]*Department of Physics, Gakushuin University, Mejiro, Toshima-Ku, Tokyo 171-8588, Japan*

[3]*Department of Applied Physics, the University of Tokyo, Hongo, Bunkyo-Ku, Tokyo 113-8656, Japan*

(Received 3 May 2002; revised manuscript received 21 February 2003; published 26 August 2003)

Through ac and thermal relaxation calorimetry techniques, we have performed a thermodynamic investigation of the spin-Peierls systems, $(DMe\text{-}DCNQI)_2Ag$ and $(DMe\text{-}DCNQI)_2Li$, where DMe-DCNQI is 2,5-dimethyl-*N*,*N*′-dicyanoquinonediimine. The fully gapped nature characteristic of the spin-Peierls (sP) ground state was confirmed by the absence of γ (T-linear) term in the low-temperature heat capacity for a single crystal. At higher temperatures, two distinct peaks were observed at 71 K and 86 K in heat capacity of $(DMe\text{-}DCNQI)_2Ag$, while only a single peak was observed at 52 K for $(DMe\text{-}DCNQI)_2Li$. The two-step structure in the Ag salt suggests that the sP transition of this material involves an intermediate state which is probably attributable to the degrees of freedom inside the dimers. For compacted pellets of numerous pieces of tiny crystals, however, the thermal anomaly around the sP transition disappears, but instead a γ term probably associated with the one-dimensional antiferromagnetic spin excitations appears. This implies that the present sP state is quite fragile against disorder or stress. These findings can be regarded as novel features of the sP transition in the quarter-filled band systems.

DOI: 10.1103/PhysRevB.68.085112 PACS number(s): 75.40.Cx, 65.40.−b, 71.20.Rv

I. INTRODUCTION

Organic charge transfer salts consisting of a strong acceptor molecule of 2,5-R_1,R_2-dicyanoquinodiimine (R_1,R_2-DCNQI),[1] and a metal cation M, have attracted attract wide interest both experimentally and theoretically, since they give various electronic phases such as metallic, charge-density-wave (CDW), charge-ordered (CO), spin-Peierls (sP), antiferromagnetic ordered ones, etc. in the quasi-one-dimensional stage. The molecular structure of R_1,R_2-DCNQI (abbreviated as DCNQI) is shown in Fig. 1. When the counter cation M is Cu, Ag, or Li, the chemical composition is expressed as $(DCNQI)_2M$ and the crystal structure is known as a tetragonal one with space group $I4_1/a$. The DCNQI molecules stack along the c axis and form a column in this direction. Each metal cation is coordinated by four neighboring DCNQI molecules belonging to different columns from distorted tetrahedral directions. The coordination angle α is an important parameter characterizing the ratio of the intra-column to inter-column transfer integrals as systematically studied in Refs. 2 and 3. The formation of a quasi-one-dimensional electronic band is predicted by the tight-binding calculations within the extended Hückel method[3] and the first-principle band calculations[4] and is confirmed by transport experiments especially for the system of $R_1=R_2=CH_3$ and $M=$Cu.

The main interests in this organic system from a viewpoint of condensed matter physics are roughly classified into two subjects. One is the hybridization effect of the π band in the DCNQI columns and d-orbital of the metal cations, as extensively studied in the last decade, for example, in $(DMe\text{-}DCNQI)_2Cu$ $(R_1=R_2=CH_3)$ and $(DI\text{-}DCNQI)_2Cu$ $(R_1=R_2=I)$ systems. Due to this hybridization effect, a drastic first-order phase transition occurs through the Mott-Hubbard mechanism of the d electrons on Cu sites cooperated with the CDW formation of the π electrons on DCNQI sites in the former salt.[5] A possibility of anomalous electron mass enhancement in the narrow π-d hybridized band is suggested by the magnetic susceptibility and heat capacity measurements in the latter salt.[6] The different magnetic characters of the one-dimensional (1D) π band and the 3D π-d hybridized band are recently unveiled by band-selective NMR experiments for these $M=$Cu salts.[7] The other interesting subject in this field is the formation of CDW and CO spin-Peierls (sP) transitions occurring in pure π-electron bands with a strongly 1D character, as is realized when M is a monovalent cation such as Ag and Li. In these salts, the competition between the bandwidth (W), electron correlation (U and V), and electron-phonon coupling gives rise to various interesting electronic phases.

In this work, we focus on $(DMe\text{-}DCNQI)_2Ag$ and $(DMe\text{-}DCNQI)_2Li$. The overlap transfer integral in the column direction ($t_\parallel$) of these salts is expected to be large among various DCNQI salts listed in Fig. 1. Even for the Ag

2,5-R_1,R_2-dicyanoquinonediimene

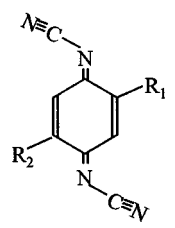

	R_1	R_2
DMe	CH_3	CH_3
DMeO	CH_3O	CH_3O
MeBr	CH_3	Br
MeCl	CH_3	Cl
BrCl	Br	Cl
DBr	Br	Br
DCl	Cl	Cl
DI	I	I

FIG. 1. Molecular structure of (R_1,R_2-DCNQI) and possible candidates for R_1 and R_2.

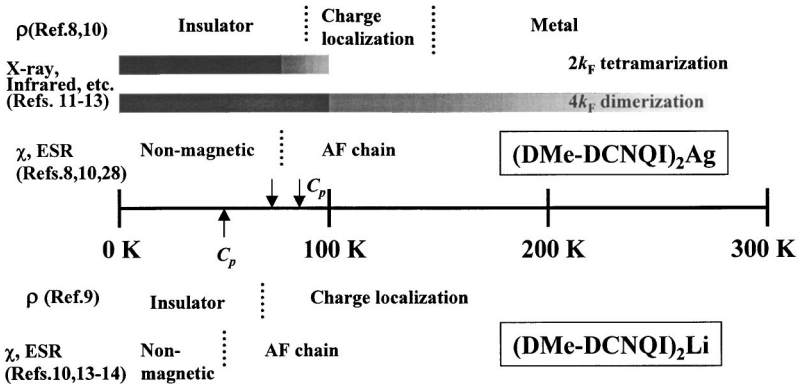

FIG. 2. A schematic view of the temperature dependence of electronic properties of $(DMe\text{-}DCNQI)_2Ag$ and $(DMe\text{-}DCNQI)_2Li$ established by transport (Refs. 8–10), magnetic susceptibility (Refs. 10, 30, and 14), ESR (Ref. 8), x-ray scattering (Refs. 11 and 12), and infrared spectroscopy (Ref. 13). Arrows labeled by C_p mean the anomalies in the heat capacity found in the present work.

salt, the d_{xy} level of Ag atoms is far below the Fermi level and takes no part in the conduction bands. Since the ionic radius of Ag is much larger than that of Li, the chemical pressure favors segregation of the neighboring columns and serves to enhance the one-dimensional character of the electronic state. In Fig. 2, we schematically summarize the physical properties below 300 K. Reflecting the 1/4 filled conduction band, the transport properties of the $(DMe\text{-}DCNQI)_2$ Ag and $(DMe\text{-}DCNQI)_2$Li are metalliclike many organic conductors consisting of BEDT-TTF or TMTSF molecules, where BEDT-TTF is bis(ethylenedithio)tetrathiafulvalene and TMTSF is tetramethyltetraselenafulvalene. The resistivity value at room temperature is reported to be about 0.02–0.10 Ω cm.[8–10] Although this value is rather large as a metallic system, the temperature dependence has a positive slope down to about 150–170 K in the Ag salt. The resistivity shows an abrupt increase below about 80–90 K recognized as a kind of metal-insulator transition. As for the Li salt, resistivity does not have any minimum below room temperature and an M-I transition occurs at about 60–80 K.[9] Careful x-ray scattering experiments for the Ag salt were performed by Moret *et al.*[11] and Nogami *et al.*[12] The development of $4k_F$ streak observed below room temperature demonstrates that the dimerization of DCNQI molecules in the stack direction gradually and dynamically grows with lowering temperatures. At about 100 K, this streak condenses into spots, indicating a charge localization with 3D correlation due to the dimerization around this temperature. Therefore, below this temperature, the $S=1/2$ spin moment localizes on each dimer. At about 83 K, another spot with the wave vector of $2k_F$ appears. The static susceptibility and ESR intensity show a drastic decrease around this temperature, demonstrating that the sP transition takes place here.[8,10] In the case of Li salt, a similar decrease of magnetic susceptibility and NMR Knight shift occurs around 50 K.[10,14] The situation in these materials is similar to the well-known organic system $[MEM\text{-}(TCNQ)_2]$,[15] in which $S=1/2$ spin localized in each TCNQ dimer undergoes a sP transition. Although sP transitions are reported in several organic salts such as $[MEM\text{-}(TCNQ)_2]$ ($T_{sP}=20$ K), TTF-BDT(M) [TTF-$MS_4C_4(CF_3)_4$, $M=$Cu ($T_{sP}=12.4$ K), Au ($T_{sP}=2.06$ K)],[16] $(TMTTF)_2PF_6$ ($T_{sP}=15$ K)[17] and also in the recently observed inorganic $CuGeO_3$ ($T_{sP}=14$ K),[18] NaV_2O_5 ($T_{sP}=35$ K) (Ref. 19) systems, the transition temperatures of the present DCNQI salts are two or three times higher than these materials. This may be related with the enhancement of magnetic coupling constant J/k_B in the stack direction by the charge degree of freedom as is suggested by Bray *et al.* in the review paper of Ref. 20.

The heat capacity measurement is a quite useful means to characterize the nature of phase transitions, since it provides quantitative information through the entropy and enthalpy changes around the transitions. The sP transition gives rise to a heat capacity peak characteristic of a second-order phase transition.[20,21] Moreover, through a thermodynamic analysis based on the low-temperature heat capacity data, one can get information about the gap structure in the magnetic excitation spectrum as was performed for typical materials mentioned above.[15,22,23] For the present DCNQI salts, however, no thermodynamic studies have been performed so far in spite of their higher transition temperatures, probably because of the difficulty to get large amount of samples with high quality. In the present work, we report results of thermodynamic measurements of these materials and discuss the nature of the sP transitions.

II. EXPERIMENT

The crystals used for this study were synthesized by the electrochemical reduction in the standard H-type cell. The typical crystals yielded are about $0.005\times0.005\times1$ mm^3 in size for Ag salt. In the case of Li salt, we used crystals from two different batches. In the first batch, we had rather thick single crystals with typical dimension of $0.2\times0.1\times1$ mm^3 and in the other batch needle-type crystals with $0.01\times0.01\times0.2$ mm^3 were available.

Heat capacity measurements were performed with a chopped-light ac calorimetry technique and a thermal relaxation technique. The temperature ranges studied were 15–300 K for the former and 0.3–230 K for the latter. We used two different apparatus to perform the relaxation calorimetry. One is the PPMS system (Quantum Design model 6000) which requires 1-2 mg for getting data in a temperature range between 2 and 230 K. We also measured the heat capacity under a magnetic field of 6 T with this apparatus. To obtain data at lower temperatures, we also used a home-built ^{3}He apparatus constructed for measuring small amount of samples weighing less than 0.5 mg. The instrumental details are already reported in Ref. 24 for the ac calorimeter and in Ref. 25 for the home-built calorimeter. Since the ac calorim-

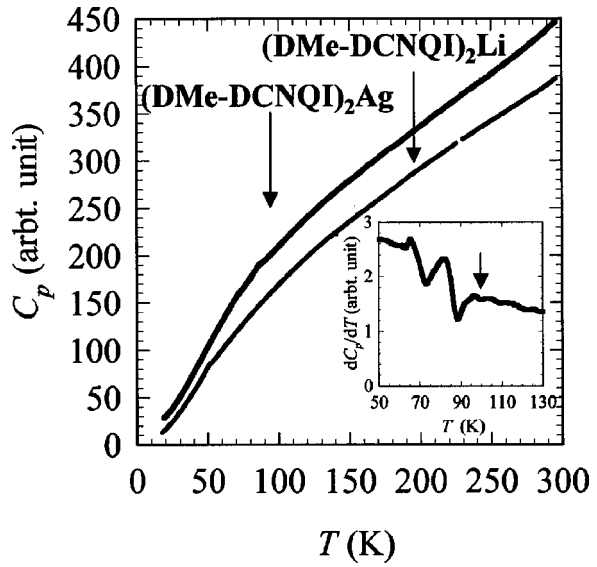

FIG. 3. Results of ac calorimetry on $(DMe\text{-}DCNQI)_2Ag$ and $(DMe\text{-}DCNQI)_2Li$. The inset shows the temperature derivative of C_p of $(DMe\text{-}DCNQI)_2Ag$. An arrow indicates the temperature below which the $4k_F$ spots appears in x-ray scattering experiments (Ref. 11).

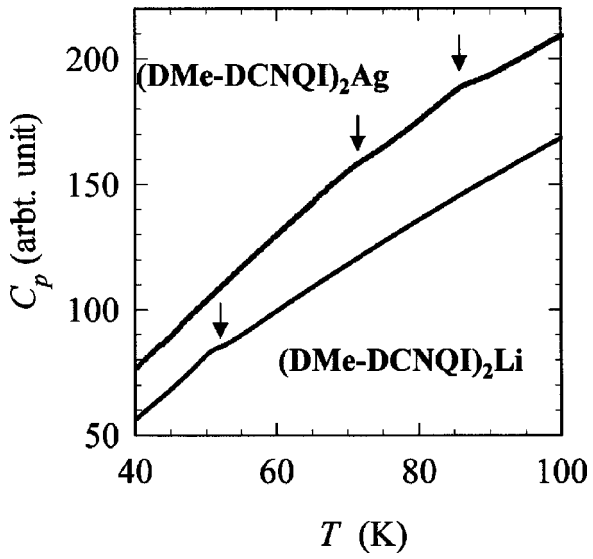

FIG. 4. Results of ac calorimetry on $(DMe\text{-}DCNQI)_2Ag$ and $(DMe\text{-}DCNQI)_2Li$ in a temperature range between 40 and 100 K.

etry has an advantage of giving high-resolution data for small amount of sample weighing about 10 μg, it is useful to detect small anomaly using one or several pieces of single crystals. Solely with this method, however, it is difficult to get absolute values of the heat capacity. Therefore, we carefully studied around the phase transition temperature by the ac technique to check the presence or absence of a thermal anomaly and to see its shape if present, while the absolute values of the heat capacity were determined by the relaxation method. In case of the relaxation calorimetry, it is basically important to realize good thermal uniformity inside a sample and good thermal contact between the sample and the sample holder. To fulfill this requirement even for the measurements of tiny crystals, we compressed numerous pieces of fine crystals into a pellet with a diameter of 2 mm and a height of 0.2–0.3 mm with a typical mass of 0.9–1.2 mg.

III. RESULTS AND DISCUSSION

A. Temperature dependence of heat capacities of $(DMe\text{-}DCNQI)_2Ag$ and $(DMe\text{-}DCNQI)_2Li$

The results of ac calorimetry for the Ag and Li salts are shown in Fig. 3. We used a bundle of several pieces of needle crystals for the measurement of the Ag salt, while one piece of single crystal is used for that of the Li salt. Since the measurements are performed at a low frequency of 1 Hz, obtained data are regarded as the static heat capacity. In fact, there is no tendency of existence of a glass transition region where a relaxation time of the relevant degree of freedom is comparable to the measuring frequency.[26] The data between 40 K and 100 K are shown in an expanded scale in Fig. 4, in which one can recognize small anomalies around 71 and 86 K for the Ag salt and at 52 K for the Li salt. The peak temperatures coincide fairly well with the temperatures where the abrupt drop of the magnetic susceptibility takes place in both salts. Therefore, the change of the magnetic property occurs as a distinct phase transition. We could neither see any symptom of latent heat nor supercooling/heating phenomena, which means the transition is of second order. The good correspondence of the heat capacity data with the magnetic property and the second order nature of the transition is consistent with the picture of a sP transition. In addition, the transition temperature 86 K of the Ag salt corresponds to the temperature of the $2k_F$ spots, demonstrating that lattice tetramerization appears in the x-ray scattering experiments by Moret *et al.*[11] The x-ray experiment also detected the appearance of $4k_F$ spots around 100 K, which shows the dimerization with interchain coherency. However, we could not see any distinct anomaly in the temperature dependence of heat capacity around this temperature. Even in the derivative (dC_p/dT) shown in the inset of Fig. 3, no kink structure was observed. Probably, the dimerization process and the concomitant charge localization reflected in the transport measurements develops below room temperatures as was suggested by Moret *et al.*[11] and this gradual and dynamical growth of dimerization does not produce anomaly in the thermodynamic sense.

The absolute heat capacity obtained by the thermal relaxation method for the Ag salt is 229.8 $J\,K^{-1}\,mol^{-1}$ at 100 K and 361.1 $J\,K^{-1}\,mol^{-1}$ at 200 K. That for the Li salt is 197.3 $J\,K^{-1}\,mol^{-1}$ at 100 K and 341.5 $J\,K^{-1}\,mol^{-1}$ at 200 K. These values seem reasonable in comparison with those of other DCNQI salts and several salts consisting of BEDT-TTF, TMTSF or TCNQ molecules. The overall temperature dependences shown in Fig. 3 are similar to that of $(DMe\text{-}DCNQI)_2$ Cu reported by Nishio *et al.*[27] Figure 5 displays the C_pT^{-1} vs T plot of the ac calorimetry data after adjusting the absolute values of C_p using the relaxation data.

In order to examine the thermal anomalies of the Ag and Li salts in detail, we determined base lines using the calibrated data in Fig. 5. It is reasonable to assume that the

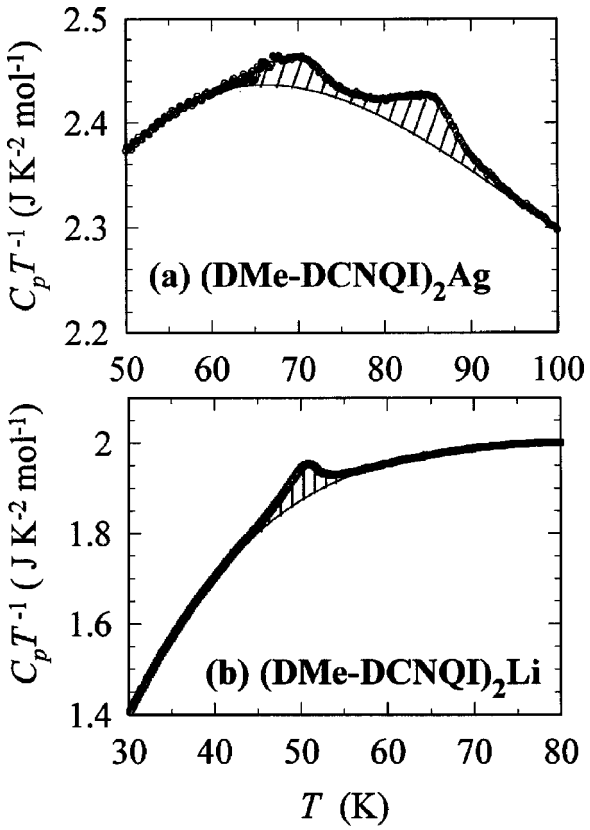

FIG. 5. C_pT^{-1} vs T plot of the ac calorimetry data after calibration of the absolute values using the thermal relaxation calorimetry data of (a) (DMe-DCNQI)$_2$Ag and (b) (DMe-DCNQI)$_2$Li. The solid curves are base lines represented by polynomial functions of the temperature (see the text). The hatched areas are used for calculation of the possible entropy gain due to the transitions.

lattice heat capacity does not give a drastic temperature dependence in such a high temperature range. Therefore, we fit the total heat capacity data in the temperature ranges of 17–25 K and 92–130 K to a polynomial function of temperature up to tenth order in the case of the Ag salt. Upon subtracting the fitted curve from the C_p data, we get the excess heat capacity around the transitions. A similar treatment was performed using the data of 16–25 and 60–80 K and the tenth order polynomials in the case of the Li salt. The heights of the heat capacity peaks at 86 and 71 K are about 2.0% and 1.2% of the absolute value of heat capacity. This amounts to 3.8% for the Li salt. The $\Delta C_pT_{sP}^{-1}$ values are $49.5\,\mathrm{mJ\,K^{-2}\,mol^{-1}}$ for the 86-K peak and $29.6\,\mathrm{mJ\,K^{-2}\,mol^{-1}}$ for the 71-K peak of the Ag salt and that for the Li salt is $74.1\,\mathrm{mJ\,K^{-2}\,mol^{-1}}$. The spin entropy in these systems should be as much as $R\ln 2$ ($\approx 5.76\,\mathrm{J\,K^{-1}\,mol^{-1}}$) per formula unit in the high temperature limit, since each spin is localized on a dimer. In addition, if the sP transition takes place, some additional entropy change originating from the change in the soft modes of lattice vibrations should be considered. The latter contribution is considered to be gradual and may be buried in the variation of base-line in the present case. The entropy gain just around the peak (hatched area in Fig. 5) gives values of 10.9% and 7.1% of $R\ln 2$ for the Ag and the Li salts, respectively, that is consistent with the sP picture, considering the effects of 1D short-range $2k_F$ tetramerization above the transition.

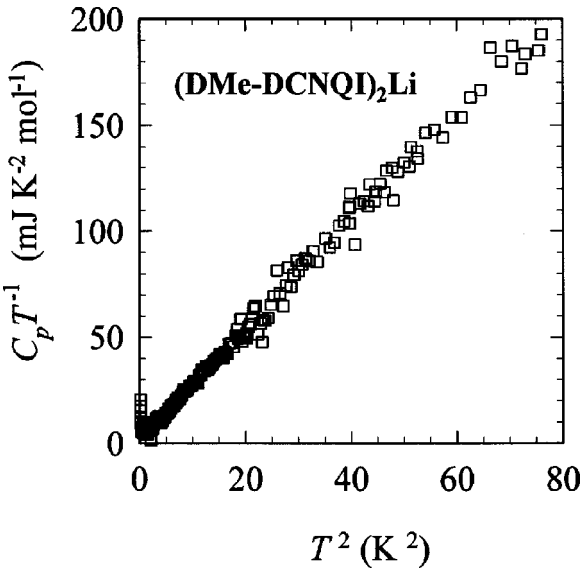

FIG. 6. C_pT^{-1} vs T^2 plot for (DMe-DCNQI)$_2$Li single crystal.

B. Magnetic excitations at low temperatures

The spin-Peierls transition is known to occur in $S=1/2$ antiferromagnetic Heisenberg chains through the magnetoelastic coupling of spin moments and the three dimensional lattice vibrations.[20,21] Below the transition temperature, progressive lattice dimerization (tetramerization in the present case because of one spin sitting on a dimer) produces an energy gap in the magnetic excitations. The ground state is a spin-singlet state and the first excited state is a triplet state. Therefore, to study the magnetic excitation spectrum through thermodynamic measurements is a persuasive means to judge whether a spin-Peierls ground state is a formed or not. In the low-temperature region far below the transition temperatures, the electronic contribution to the heat capacity should have an exponential dependence on temperature owing to the formation of an energy-gap (Δ) in the magnetic excitation spectrum, just as in the case of the superconductivity of an *s* wave. In fact, [MEM-(TCNQ)$_2$] (Ref. 15) and TTF-BDT*M* (Ref. 20) are analyzed based on the mean field approach using the coefficient (γ) of the T-linear term of the heat capacity, which originates from the 1D antiferromagnetic (AF) spin-wave excitations.

To confirm whether the gap is really opened or not, we performed low-temperature measurement using a thick single crystal with $0.2\times 0.15\times 2.0\ \mathrm{mm^3}$ and 0.20 mg for the Li salt. We cut this crystal into three pieces and attached them to the sample holder. To avoid the inhomogeneous pressure effect produced by adhesion, we covered only a part of the bottom surface of each piece by small amount of Apiezon N grease. The obtained data are shown in Fig. 6 in a C_pT^{-1} vs T^2 plot. If we assume that the low-temperature behavior of the lattice part below 3.4 K is described by a simple Debye theory, it is possible to perform a linear ex-

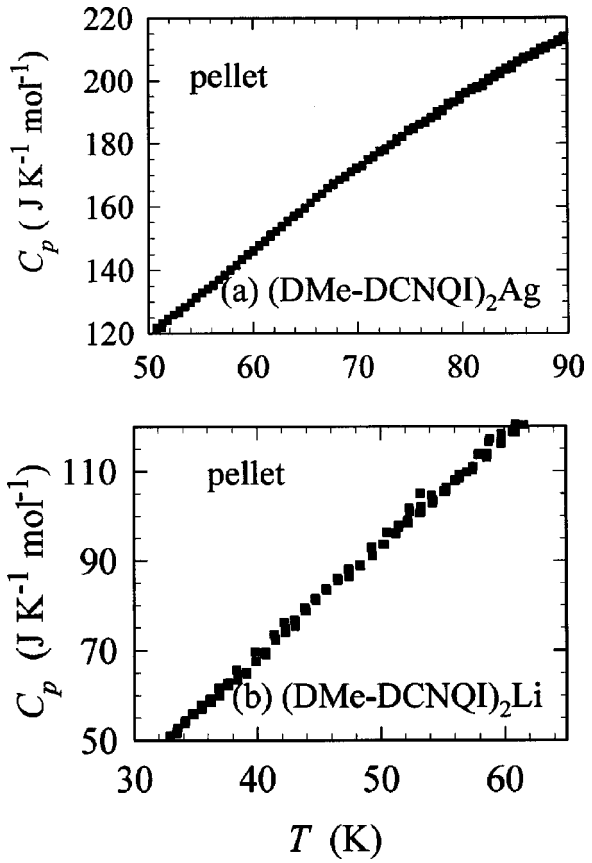

FIG. 7. Heat capacities around the sP transitions of pellet samples of (a) (DMe-DCNQI)$_2$Ag and (b) (DMe-DCNQI)$_2$Li.

trapolation of C_pT^{-1} vs T^2 curve down to 0 K. As is seen in the figure, this extrapolation gives a vanishing γ term in the heat capacity. This result ensures that there is a distinct gap in the magnetic excitations as is expected for the spin-Peierls ground state.

The low-temperature heat capacity measurements are also performed for compacted pellet samples of tiny crystals of which total weight is 120μg,80μg for the Ag salt and 0.87 mg for the Li salt. Unlike the single crystal data shown in Fig. 6, the behavior at low temperatures seems to give larger values. For the Li salt, the linear extrapolation of the C_pT^{-1} vs T^2 curve down to 0 K gives a finite γ term of 11.3 mJ K^{-2} mol^{-1}. In the case of the Ag salt, we have observed that the γ value reaches about 25–32 mJ K^{-2} mol^{-1}, although appearance of slight upturn of C_pT^{-1} at the lowest temperatures and a low Debye temperature prohibit us from determining accurate γ value by the simple linear extraporation of the C_pT^{-1} vs T^2 curve. The data around the sP transitions for the pellet samples are shown in Figs. 7(a) and (b). Surprisingly, the peak structure associated with the sP transition, which was clearly observed in Figs. 3 and 4, disappears. It is considered that the lattice distortion induced by the inhomogeneous stress inevitably produced in the process of pellet-formation seriously affects the formation of the spin-Peierls state. It is well known that the spin-Peierls system is very sensitive to the external pressure and small amount of impurities, as is extensively studied in $CuGeO_3$.[21]

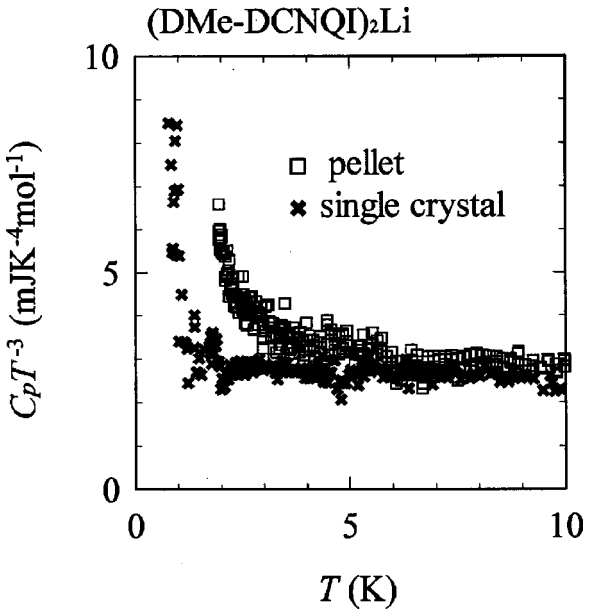

FIG. 8. C_pT^{-3} vs T plots of a (DMe-DCNQI)$_2$Li single crystal and a pellet.

The interesting contrast with $CuGeO_3$ is that no Néel ordering or spin-glass state takes place in the present DCNQI systems. The γ term induced in the pellet is considered as an indication of 1D AF spin-wave excitations, since the C_pT^{-3} vs T plot of the Li salt shown in Fig. 8 clearly shows that the β term due to the lattice heat capacity is the same in the single crystal and the pellet samples. The picture of 3D spin wave excitations in the antiferromagnetically ordered state is, thus, excluded by this experiment.

C. Analysis of the peak structure based on the mean-field approach

Using the γ value obtained by the low-temperature experiments, we perform a mean-field analysis for the heat capacity data around the transition of the Li salt, which seems to give a typical sP character. At first, we assume that C_p is expressed as

$$C_p = C_{\text{lattice}} + C_{1\text{D}} + \Delta C_p , \tag{1}$$

where C_{lattice} is the lattice heat capacity, $C_{1\text{D}}$ is the magnetic heat capacity of 1D AF spin chains, and ΔC_p is the excess contribution due to the spin-Peierls transition. In the analysis, $C_{1\text{D}}$ is assumed to be a step function which is zero below T_{sP} ($=52$ K), above this temperature, it should show the so-called Bonner-Fisher-type temperature dependence. In the low-temperature limit it is expressed as $C_{1\text{D}} = 0.35Rk_BT/|J|$ (J being an intrachain magnetic coupling in the Bonner-Fisher model).[28] Assuming that the pellet samples without a spin-Peierls transition carry the 1D AF spins even down to the lowest temperatures measured, we estimated possible J/k_{B}'s using the γ values of the pellet and got C_{1D} curves above T_{sP}. The obtained value is $J/k_B = -257$ K. It is reasonable to consider that C_{lattice} gives a smooth temperature dependence expressed by the same order

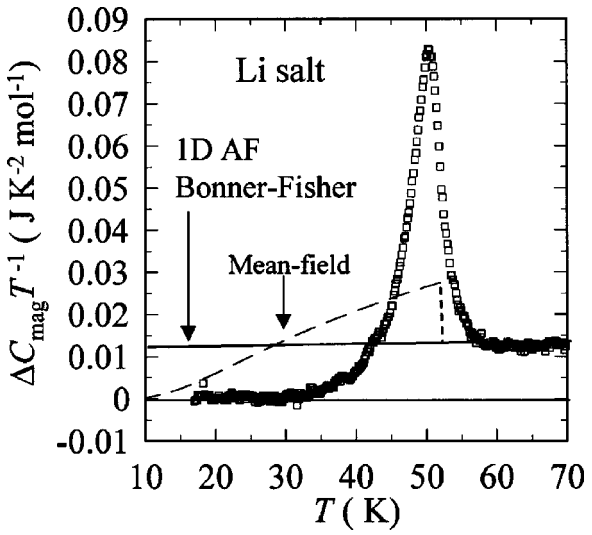

FIG. 9. Mean-field analyses of the thermal anomalies associated with the spin-Peierls transition of $(DMe\text{-}DCNQI)_2Li$. The dashed curves show possible mean-field peak of the spin-Peierls transition and solid curves represent heat capacities of the antiferromagnetic $S=1/2$ chains (Ref. 28).

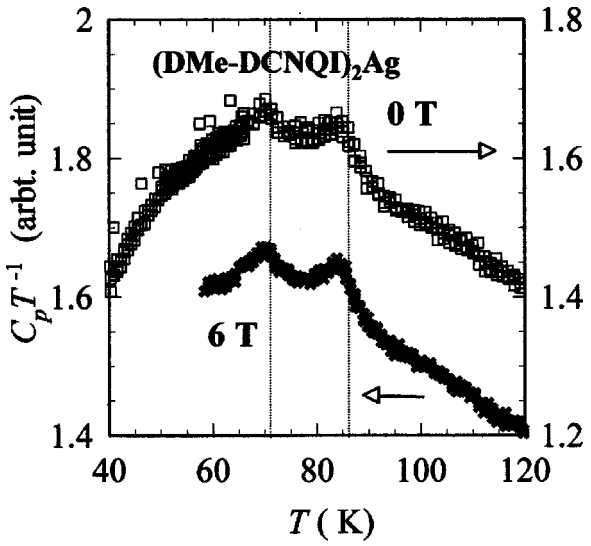

FIG. 10. Peak structures around the spin-Peierls transitions of $(DMe\text{-}DCNQI)_2Ag$ obtained by thermal relaxation calorimetry under magnetic fields of 0 and 6 T.

of polynomial functions (up to the tenth order) as we have selected to determine the background curve in the discussion of 3.1. Using the experimental data of C_p in the temperature ranges 16–25 K, and 65–90 K, we can derive magnetic heat capacity, $\Delta C_{\rm mag}=\Delta C_p+C_{\rm 1D}$ as a function of temperature. The result is shown in Fig. 9 in a form of $\Delta C_{\rm mag}T^{-1}$ vs T plot. The dashed curves are the mean-field curves based on the analogy of BCS weak-coupling theory, and the solid curves an the Bonner-Fisher heat capacities. The deviation of the data points from the mean-field curve is apparent, especially in the height and the shape of the peak. This shows a contrast with the case of [MEM-$(TCNQ)_2$], in which the sP peak can be well described by the analogy of the BCS framework with $\Delta C_p {T_{sP}}^{-1}=1.43\gamma$.[15] We infer that the strong electron-phonon interaction and enhanced 1D character in this organic salt induce strong fluctuations and gives rise to the large discrepancy from the mean-field peak, especially the peak height. It should be emphasized, however, that the entropy balance between $\Delta C_{\rm mag}T^{-1}$ curve and the Bonner-Fisher curve shown in Fig. 9 seems satisfactory as far as the ambiguity involved in determining the $C_{\rm lattice}$ term is taken into account. The value of $J/k_{\rm B}=-257$ K is comparable to the reported value of -205 K obtained by the magnetic susceptibility analysis performed by Sakurai *et al.*[29] Based on this $J/k_{\rm B}$ value, the possible magnetic entropy at 52 K $(=T_{SP})$ can be estimated as $0.06R$ through the Bonner-Fisher model in Ref. 28. The close correspondence between this value and the entropy associated with the thermal anomaly shown in Fig. 5 together with the good entropy balance in Fig. 9 guarantee the correctness of the thermodynamic framework based on the sP transition in this salt.

It is difficult to perform a similar analysis for the Ag salt, since the C_pT^{-1} at low temperatures implies additional contributions other than 1D spin excitations as we have mentioned in Sec. III B. Although the J/k_B value estimated from the temperature dependence of the susceptibility data in Refs. 10 and 30 is -244 K which is close to that of the Li salt, the rather large but reproducible γ value for this salt is somewhat curious. This result may imply the qualitative difference of the sP character of this salt, which will be discussed in the next section.

D. Anomalous two-step peak of the ag salt

Here, we discuss the curious two-step structure of the thermal anomaly observed in the Ag salt. It is quite unusual that the sP transition shows two peaks in the heat capacity curve. By the ac calorimetry, we checked the thermal anomaly for samples from different batches. However the peak temperatures and peak shape were reproducible in all the measurements. In Fig. 10, we plotted the data of C_pT^{-1} obtained by the thermal relaxation calorimetry. In this measurement the sample is a bundle of tiny crystals adhered on the sample holder by Apiezon *N* grease. Since the thermal coupling between the crystals is not good enough to ensure the absolute value, we do not label the absolute values in the vertical axis. The peak structure was well reproduced by this method. Therefore, we conclude that the two step transition is intrinsic in this material. In this salt, the drop of magnetic susceptibility occurs over a wider temperature region than that of the Li salt.[30] This behavior is consistent with the present thermodynamic observation, because the Ag salt falls into a nonmagnetic state through the two-step process. The existence of two distinct peaks suggests the presence of an intermediate state in the process of a sP transition of the Ag salt. The C_pT^{-1} data obtained under a magnetic field of 6 T are also shown in Fig. 10. The peculiar aspect of the present sP transition is that the spin moment is localized on a DCNQI *dimer* and falls into a nonmagnetic state in the lattice tetramerization process. In this sense, this salt can have a

degree of freedom in the distribution of charges and spins inside the dimers and such freedom coupled with the intracolumn transfer ($t_{\|}$) may give an unprecedented intermediate state during the transition. In the case of $(DI\text{-}DCNQI)_2Ag$, the charge ordering (CO) due to the nearest neighbor Coulomb repulsion (V) is reported in the same crystal structure but has a narrower electronic band,[31,32] This suggests that even in the present material the nearest-neighbor effects inside the dimers should be taken into account to explain the overall phenomena. It is not unreasonable that if the present system is marginal for the charge ordering, some kind of charge disproportionation can be triggered by the lattice modulation associated with the sP transition. As a matter of fact, recent ^{13}C-NMR experiments clearly observed the existence of such a kind of intermediate state, probably originating from the intradimer effect.[33] This result implies interesting aspects, and possibly a further variation of sP transition in organic systems which have various kinds of freedom in the molecular arrangements, and so on. The unexpectedly large C_pT^{-1} values observed in the low-temperature experiment may be related with this unusual sP state coupled with charge degree of freedom. The description of the ground state in which the CO and sP mechanisms coexist is still an open question, but subject to extensive study both experimentally and theoretically these days.[34,35]

IV. SUMMARY

We experimentally studied the thermodynamic properties of $(DMe\text{-}DCNQI)_2Ag$ and $(DMe\text{-}DCNQI)_2Li$. Although the Li salt showed a single peak at 52 K, the Ag salt exhibited two thermal anomalies at 71 and 86 K. The magnitude of the heat capacity jump (ΔC_p) was consistent with the spin-Peierls picture. The double peak observed in the Ag salt indicates the presence of an intermediate state during the spin-Peierls transition due to the degrees of freedom inside the dimer. The low-temperature heat capacity obtained for a single crystal sample demonstrates that the ground state has a distinct gap in magnetic excitations. In compacted pellet samples, the thermal anomalies disappeared, but instead a γT term mainly attributable to the 1D antiferromagnetic spin wave appeared. This is interpreted as the stress and/or disorder effect on the spin-Peierls transition in DMe-DCNQI compounds..

ACKNOWLEDGMENTS

This work was financially supported in part by a Grant-in-Aid for Scientific Research No. 11640362 from the Ministry of Education, Culture, Sports, Science, and Technology, Japan. One of the authors (Y.N.) also thanks the Toyota Physical and Chemical Research Institute for financial support.

*Present address: Dept. of Chemistry, Tokyo Institute of Technology, O-okayama, Meguro-Ku, Tokyo 152-8551, Japan.

†Present address: Dept. of Organic and Polymeric Materials, Tokyo Institute of Technology, O-okayama, Meguro-Ku, Tokyo 152-8552, Japan.

[1] A. Aumüller, P. Erk, G. Klebe, S. Hünig, J. U. von Schütz, and H. P. Werner, Angew. Chem., Int. Ed. Engl. **25**, 740 (1986).

[2] R. Kato, Bull. Chem. Soc. Jpn. **73**, 515 (2000).

[3] A. Kobayashi, R. Kato, H. Kobayashi, T. Mori, and H. Inokuchi, Solid State Commun. **64**, 45 (1987); R. Kato, H. Kobayashi, and A. Kobayashi, J. Am. Chem. Soc. **111**, 5224 (1989).

[4] T. Miyazaki, K. Terakura, Y. Morikawa, and T. Yamasaki, Phys. Rev. Lett. **74**, 5104 (1995); T. Miyazaki and K. Terakura, Phys. Rev. B **54**, 10 452 (1996).

[5] H. Fukuyama, J. Phys. Soc. Jpn. **61**, 3452 (1992); *Correlation Effects in Low-Dimensional Electron Systems*, edited by A. Okiji and N. Kawakami (Springer, New York, 1994), p. 128.

[6] M. Tamura, Y. Kashimura, H. Sawa, S. Aonuma, R. Kato, and M. Kinoshita, Solid State Commun. **93**, 585 (1990); Y. Nakazawa, M. Seki, K. Saito, K. Hiraki, T. Takahashi, K. Kanoda, and M. Sorai, Phys. Rev. Lett. **88**, 076402 (2002).

[7] A. Kawamoto, K. Miyagawa, and K. Kanoda, Phys. Rev. Lett. **87**, 107602 (2001).

[8] H.-P. Werner, J. U. von Schütz, H. C. Wolf, R. Kremer, M. Gehrke, A. Aumüller, P. Erk, and S. Hünig, Solid State Commun. **65**, 809 (1988).

[9] T. Yamamoto, H. Tajima, J. Yamaura, S. Aunuma, and R. Kato, J. Phys. Soc. Jpn. **68**, 1384 (1999).

[10] K. Hiraki, Ph.D Thesis, The Graduate University for Advanced Studies, 1996.

[11] R. Moret, P. Erk, S. Hünig, and J. U. von Schütz, J. Phys. (France) **49**, 1925 (1988).

[12] Y. Nogami, K. Oshima, K. Hiraki, and K. Kanoda, J. Phys. IV **9**, Pr10-357 (1999).

[13] M. Meneghetti, G. Lunardi, R. Bozio, and C. Pecile, Synth. Met. **41–43**, 1775 (1991).

[14] K. Miyagawa, A. Kawamoto, and K. Kanoda, Phys. Rev. B **60**, 14 847 (1999).

[15] S. Huizinga, J. Kommandeur, G. A. Sawatzky, B. T. Thole,K. Kopinga, W. J. M. de Jongh, and J. Roos, Phys. Rev. B **19**, 4723 (1979).

[16] I. S. Jacobs, J. W. Bray, H. R. Hart, Jr., L. V. Interrante, J. S. Kasper, G. D. Watkins, D. E. Prober, and J. C. Bonner, Phys. Rev. B **14**, 3036 (1976).

[17] A. Maaroufi, S. Flandrois, G. Fillion, and J. P. Morand, Mol. Cryst. Liq. Cryst. **119**, 311 (1985).

[18] M. Hase, I. Terasaki, and K. Uchinokura, Phys. Rev. Lett. **70**, 3651 (1993).

[19] M. Isobe and Y. Ueda, J. Phys. Soc. Jpn. **65**, 1178 (1996).

[20] J. W. Bray, L. V. Interrante, I. S. Jacobs, and J. C. Bonner, in *Extended Linear Chain Compounds*, edited by J. S. Miller (Plenum Press, New York, 1983), Vol. III.

[21] J. C. Bonner and H. W. J. Blöte, Phys. Rev. B **25**, 6959 (1982).

[22] T. Wei, A. J. Heeger, M. B. Salamon, and G. E. Delker, Solid State Commun. **21**, 595 (1977).

[23] S. B. Oseroff, S.-W. Cheong, B. Aktas, M. F. Hundley, Z. Fisk, and L. W. Rupp, Jr., Phys. Rev. Lett. **74**, 1450 (1995); X. Liu, J. Wosnitza, H. v. Lohneysen, and R. K. Kremer, *ibid.* **75**, 771 (1995).

[24] K. Saito, Y. Yamamura, and M. Sorai, Netsu Sokutei (Calor. Therm. Anal.) **25**, 150 (1998).

[25] Y. Nakazawa, A. Kawamoto, and K. Kanoda, Phys. Rev. B **52**, 12 890 (1995).

[26] H. Akutsu, K. Saito, Y. Yamamura, K. Kikuchi, H. Nishikawa, I. Ikemoto, and M. Sorai, J. Phys. Soc. Jpn. **68**, 1968 (1999); H. Akutsu, K. Saito, and M. Sorai, Phys. Rev. B **61**, 4346 (2000).
[27] Y. Nishio, M. Tamura, K. Kajita, S. Aonuma, H. Sawa, R. Kato, and H. Kobayashi, J. Phys. Soc. Jpn. **69**, 1414 (2000).
[28] J. C. Bonner and M. E. Fisher, Phys. Rev. **135**, A640 (1964).
[29] T. Sakurai, H. Ohta, S. Okubo, K. Kanoda, and K. Hiraki, Synth. Met. **120**, 851 (2001).
[30] K. Hiraki and K. Kanoda, Synth. Met. **86**, 2103 (1997).
[31] K. Hiraki and K. Kanoda, Phys. Rev. Lett. **80**, 4737 (1998).
[32] H. Seo and H. Fukuyama, J. Phys. Soc. Jpn. **66**, 1249 (1997).
[33] K. Hiraki and K. Kanoda (unpublished).
[34] M. Kuwabara, H. Seo, and M. Ogata, J. Phys. Soc. Jpn. **72**, 225 (2003).
[35] K. C. Ung, S. Mazumdar, and D. Toussaint, Phys. Rev. Lett. **73**, 2603 (1994).